2014

Numerical Model of Capillary Tubes: Enhanced Performance and Study of Non-Adiabatic Effects

Nicolas Ablanque
Centre Tecnològic de Transferència de Calor (CTTC), Universitat Politècnica de Catalunya (UPC), nicolas@cttc.upc.edu

Carles Oliet
Centre Tecnològic de Transferència de Calor (CTTC), Universitat Politècnica de Catalunya (UPC), carles@cttc.upc.edu

Joaquim Rigola
Centre Tecnològic de Transferència de Calor (CTTC), Universitat Politècnica de Catalunya (UPC), quim@cttc.upc.edu

Carlos David Pérez-Segarra
Centre Tecnològic de Transferència de Calor (CTTC), Universitat Politècnica de Catalunya (UPC), segarra@cttc.upc.edu

Numerical Model of Capillary Tubes: Enhanced Performance and Study of Non-Adiabatic Effects

Nicolás ABLANQUE[1]*, Carles OLIET[1], Joaquim RIGOLA[1], Carlos-David PEREZ-SEGARRA[1]

[1]Universitat Politècnica de Catalunya – BarcelonaTech (UPC), Heat and Mass Transfer Technological Center (CTTC),Terrassa, Barcelona,Spain
(+34 937398192, +34 937398920, www.cttc.upc.edu)

* Corresponding Author

ABSTRACT

In the present work a numerical model to simulate the thermal and fluid-dynamic phenomena inside non-adiabatic capillary tubes is presented. It consists of an improved version of the distributed model detailed in Ablanque *et al.* (2010). The model is based on a pseudo-homogeneous two-phase flow model where the governing equations (continuity, momentum, energy and entropy) are integrated over the discretized fluid domain and solved by means of a step-by-step scheme. The main novelty of the improved algorithm is its enhanced capability to address common convergence issues typically found in distributed models for non-adiabatic capillary tubes (i.e. flow discontinuities caused by the refrigerant re-condensation). In addition, the newest version of the model allows the simulation of both concentric and lateral configurations.
This work presents the detailed numerical aspects of the new model, the implementation and validation of the lateral configuration, and a detailed study of its performance when addressing the aforementioned numerical difficulties.

1. INTRODUCTION

Capillary tubes are commonly used as the expansion device in domestic refrigerators and window air conditioners. They are pressure-reducing devices whose main role is to regulate the system refrigerant flow according to load demand. Although a capillary tube is basically a small-diameter tube connecting the condenser/gas-cooler to the evaporator, the fluid-dynamic and thermal phenomena occurring inside are very complex (phase transitions, non-equilibrium effects, heat transfer, compressibility). In these applications capillary tubes are usually in contact with the compressor suction line so that heat is transferred from the former to the latter in order to prevent liquid refrigerant from entering into the compressor. The capillary-tube/suction-line heat exchanger is commonly found in two different configurations: lateral or concentric.

The capillary tube numerical models are usually based on three different approaches (empirical, lumped and distributed). The empirical models consist of simple equations fitted from experimental data but lacking physical foundations (Sarker and Jeong, 2012). Their response is instantaneous but their out-of-range reliability is questionable. In the lumped models the capillary tube system is divided into macro zones where semi-analytical methods are applied. Each of the defined zones has different phenomenological characteristics and considerations. In the distributed approaches the domain is divided in several control volumes where the main governing equations (continuity, momentum and energy) are applied (Bansal and Yang, 2005). This type of model is time consuming with respect to the simpler methods but it provides better accuracy, higher level of detail and greater adaptability to different geometric and operational conditions.

It has been observed that the distributed models present convergence issues in non-adiabatic capillary tubes due to flow discontinuities caused by the re-condensation of the refrigerant within the heat exchange region (Khan *et al.*, 2009). The distributed model presented by Negrao and Melo (1999) was found to be conditionally convergent. It was noticed that the model discontinuities appeared in particular situations where the slope of the refrigerant flow pressure became very close to the saturation pressure profile. In order to overcome these difficulties an extrapolation

was suggested. Similar numerical problems were detected by Bansal and Xu (2003). It was found that a strong heat transfer effect caused the refrigerant to re-condense within the heat exchanger region and therefore, the refrigerant entered to the capillary tube outlet adiabatic region as sub-cooled liquid. In such cases the critical state could only be calculated for capillary tubes with long outlet adiabatic sections (capillary tubes with strong heat transfer and short outlet adiabatic section presented convergence instabilities).

It has been noticed that similar convergence problems were occurring in the model by Ablanque *et al.* (2010). Therefore, a painstaking revision of the model mathematical resolution procedure has been carried out in order to address these difficulties. The present work is focused on reviewing the major changes and modifications done to the model which have greatly improved the model convergence stability.

In the second Section of this work a brief explanation of the general formulation and resolution procedure of the model presented in Ablanque *et al.* (2010) is given together with a description of the new resolution procedures and features of the enhanced algorithm that allow a better convergence performance. The third Section is devoted to the implementation and validation of the lateral configuration (the concentric configuration has already been validated). In the fourth Section the predictions of the new model are compared against simulations carried out with other distributed models proposed in the open literature. The comparison shows that the new model succeeds (convergence is attained) in cases where high convergence difficulties have been reported.

2. MATHEMATICAL MODEL

The modeling of the capillary tubes is based on an in-tube two-phase flow numerical model and an iterative resolution procedure used to find the critical conditions.

2.1 Two-Phase Flow Model

The two-phase flow thermal and fluid-dynamic behavior inside tubes is obtained from the integration of the fluid governing equations along the flow domain (which is split into a number of finite control volumes as shown in Figure 1). Considering a steady-state quasi-homogeneous fully-implicit one-dimensional model, the discretized governing equations (continuity, momentum, energy and entropy generation) show the following form:

$$\dot{m}_i - \dot{m}_{i-1} = 0 \tag{1}$$

$$\dot{m}_i v_i - \dot{m}_{i-1} v_{i-1} = (p_{i-1} - p_i) S - \bar{\tau} \pi D \Delta z_i - \bar{\rho}_i g \sin(\theta) S \Delta z_i \tag{2}$$

$$\dot{m}(h_i + e_{c,i} + e_{p,i}) - \dot{m}_{i-1}(h_{i-1} + e_{c,i-1} + e_{p,i-1}) = \bar{\dot{q}}_i \pi D \Delta z_i \tag{3}$$

$$\dot{m}_{i-1} s_{i-1} + \dot{m}_i s_i - (\bar{\dot{q}} / T_{wall}) \pi D \Delta z_i = \dot{s}_{gen,i} \tag{4}$$

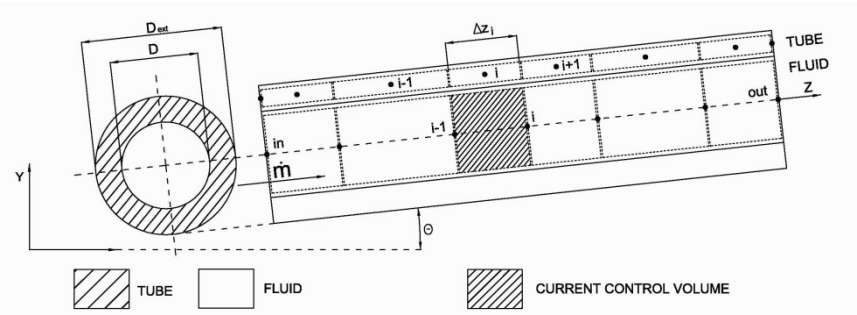

Figure 1: Fluid and solid tube discretization scheme.

The whole flow domain is solved on the basis of a step-by-step numerical implicit scheme. The main Equations (1, 2, 3 and 4) are rearranged and solved for the *i* position. Then, from the duct flow inlet conditions, namely, pressure, enthalpy and mass flow rate, each control volume outlet state is calculated sequentially. The formulation requires the use of empirical correlations to evaluate three specific parameters: the void fraction (Premoli *et al.*, 1970), the shear

stress (Churchill, 1977, and Friedel, 1979) and the convective heat transfer coefficient (Gnielinski, 1976, and Shah, 1979).

In non-adiabatic conditions, the energy balance over the solid part of the tube is also considered. The tube is discretized in a way that for each fluid flow control volume there is a corresponding tube temperature (see Figure 1). The balance takes into account the heat exchanged with the internal fluid and the heat transferred to/from an external boundary condition (e.g. an external heat transfer coefficient, an external fluid flow solved in the same way as the internal fluid, an insulation cover discretized in a two-dimensional way, etc.). The set of the algebraic equations of the solid domain are solved by means of a node-by-node method (Gauss-Seidel) or a direct method (TDMA).

The process of solving in a segregated way the inner fluid, the solid tube and the external condition (if necessary), is carried out iteratively until a converged solution is obtained. The tube wall temperature map acts as the boundary condition for the whole internal flow. The solution is given when all the variables (mass flow rate, pressure, enthalpy, tube temperatures and external variables) agree with the convergence criteria.

More complex configurations can be simulated with this algorithm. In the case of a double tube heat exchanger, four different domains are defined: i) the inner fluid (discretized and solved with the step-by-step resolution procedure); ii) the inner tube (discretized in a one-dimensional way and solved with the TDMA method); iii) the counter flow secondary fluid (discretized and solved with the step-by-step resolution procedure); and iv) the outer tube which may include an insulation cover and different materials (discretized in a two-dimensional way and solved by means of a line-by-line TDMA method). In the case of a tube soldered to another tube, three different domains are defined: i) the inner fluid of one tube, ii) the solid part (including both tubes) and iii) the inner fluid of the secondary tube.

2.2 Capillary Tube Resolution Procedure

The mass flow rate inside a capillary tube increases as the discharge pressure decreases but only up to a critical value from which the mass flow rate remains constant. This critical condition occurs when the entropy generation equation is not fulfilled in the last control volume of the tube. In the work presented by Ablanque *et al.* (2010) a particular strategy to iteratively find the critical conditions of a capillary tube with particular geometry and boundary conditions has been described. The method was based on the two-phase flow model presented in the previous Section.

However, so far the model presented similar convergence issues as those reported in the literature, therefore, a painstaking study of the numerical aspects that may improve the model convergence has been carried out by the authors. In the following list the major modifications done to the model of Ablanque *et al*. (2010) are described. The aim of all the modifications applied to the model was to avoid all kind of discontinuities (e.g. in the thermal field, in the numerical discretization, and in the numerical resolution procedure).

- *Resolution methodology.* An updated version of the non-adiabatic capillary tube resolution scheme has been implemented. The new scheme is based on a different sequential analysis (the critical condition of the capillary tube is now calculated in every iteration of the solid temperature map).
- *Axial heat transfer*. The axial heat transfer through the solid tube is now taken into account.
- *Heat transfer coefficients*. Transitional zones are now considered for the empirical correlations.
- *Common non-uniform grid*. The non-uniform grid is used along the whole capillary tube domain.

In addition, the model allows the simulation of two different capillary-tube/suction-line heat exchanger configurations which are commonly found: concentric and lateral (see Figure 2).

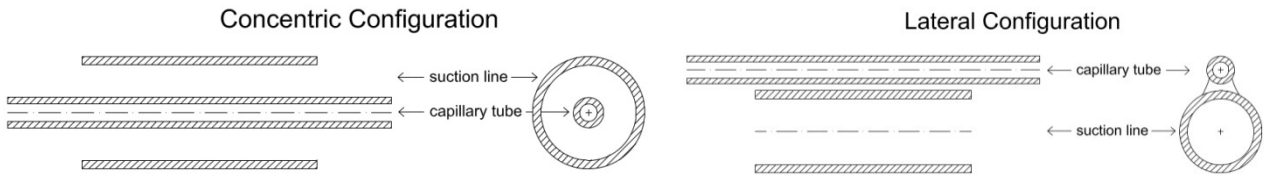

Figure 2: Typical configurations of capillary-tube/suction-line heat exchangers.

3. MODEL VALIDATION: NON-ADIABATIC LATERAL CONFIGURATION

The model presented in Section 2 has already been successfully validated for both adiabatic capillary tubes and non-adiabatic concentric capillary tubes (Ablanque *et al.*, 2010). In this work the model validation is extended to non-adiabatic lateral configurations.

Mendoça *et al.* (1998) presented experimental data of non-adiabatic capillary tubes working with refrigerant HFC-134a (see Table 1). In their work, two different capillary tube inner diameters were considered (0.61 and 0.83 mm) with an uncertainty of +/- 0.02 mm. This uncertainty has been considered for the numerical simulations (see error bars in Figure 3). The results suggest that acceptable agreement is obtained for the experimental data carried out with the larger diameter (the predictions fall within +/- 8% of the experimental data). However, the experimental data with the smaller diameter has been over-predicted by the model possibly due to the cited uncertainty and/or the fact that the roughness value was not reported. It is worth to notice that García-Valladares (2007) did not consider these experimental results for its model validation because of similar reasons.

Table 1: Lateral capillary-tube/suction-line heat exchanger experimental data information

	Fluid	D [mm]	L [m]	L_{ex} [m]	L_{in} [m]	p_{in} [bar]	T_{evap} [ºC]	ΔT_{sub} [ºC]	$T_{in,sec}$ [ºC]	ξ [μm]
Mendoça *et al.* (1998)	134a	0.83	4.001	1.597	0.533	9/14	-22.2 to -19.7	5.7 to 10.1	-17.8 to -7.3	1.5*
				1.605	1.067		-23.2 to -22.6	4.9 to 10.1	-13.5 to -5.9	
		0.61	4	1.6	1.067		-23 to -22.9	5.5 to 10.1	0.9 to 4	
				1.599	0.534		-22.6 to -3	4.8 to 10	-13.7 to 6.4	
Peixoto (1995)	134a	0.787	2.06	1	0.53	12.5/14	-10.09	2.6 to 18.7	-0.6/-3.7	0.45

*value used by García-Valladares (2007)

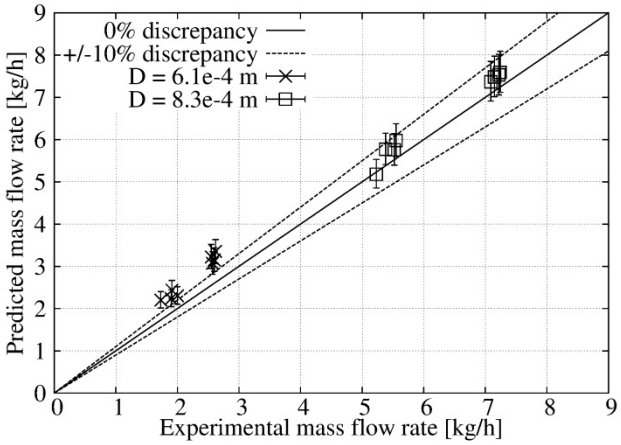

Figure 3: Numerical results against experimental data of Mendoça et al. (1998): mass flow rates.

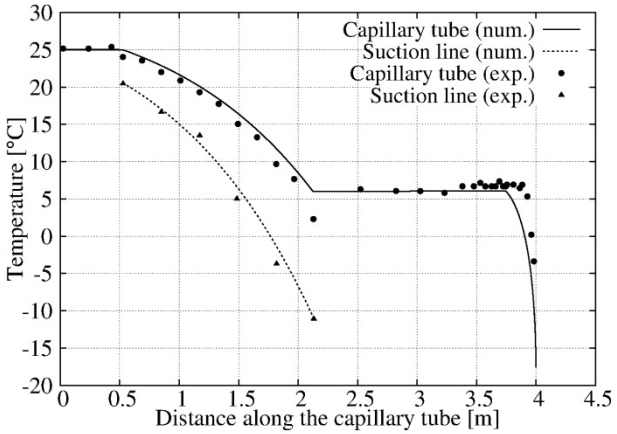

Figure 4: Numerical results against experimental data of Mendoça et al. (1998): temperature profiles.

An additional comparison is shown in Figure 4 where the temperature profiles along a whole lateral capillary tube-suction line heat exchanger are observed. Both the capillary tube and the suction line refrigerant temperature profiles are reasonably well predicted by the model.

Peixoto (1995) carried out experimental tests with HFC-134a and a non-adiabatic capillary tube of the lateral configuration. Two different condensing pressures were considered, 12.5 and 14 bar, with secondary flow inlet temperatures of -0.6 and -3.7 ºC, respectively. More details of the geometric characteristics are found in Table 1. The model numerical predictions are compared to the experimental data in Figure 5 (a high degree of agreement is achieved).

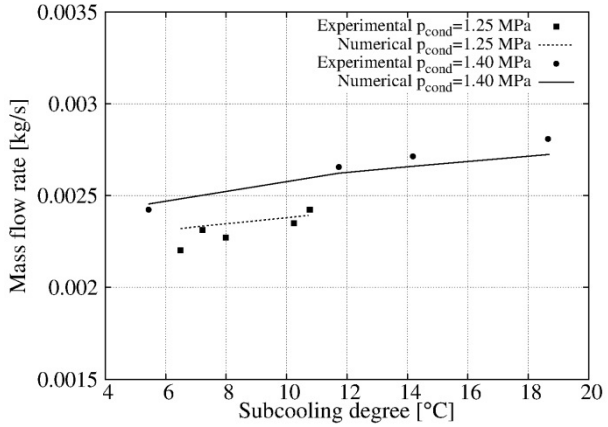

Figure 5: Numerical results against experimental data of Peixoto (1995): mass flow rates.

4. RESULTS

The distributed models presented in the technical literature (e.g. Negrao and Melo, 1999 and Bansal and Yang, 2005) have reported convergence difficulties in some particular situations (when both the refrigerant pressure slope is very close to the saturation line profile and when the last section of the capillary tube is relatively short). This problem has also been observed in the model presented by Ablanque *et al*. (2010) as shown in Figure 6. It is observed that during the search for the critical mass flow rate it may happen that for a slight variation of the mass flow rate the capillary tube solution jumps from a case where no choked condition is found (case a) to a case where the choked condition occurs somewhere inside the heat exchanger (case b). In such case the numerical algorithm is unable to find the critical mass flow rate (i.e. choked flow at the last control volume of the capillary tube).

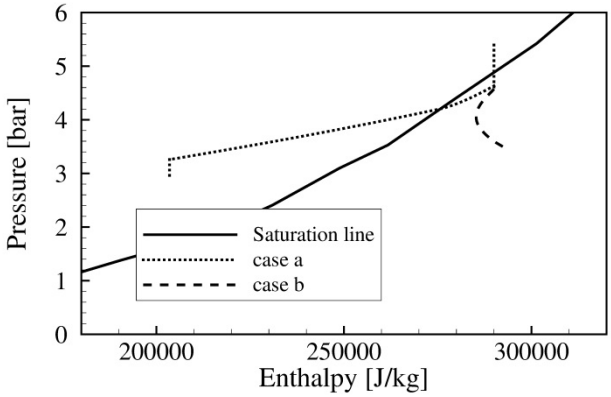

Figure 6: Resolution discontinuity: (a) mass flow rate: 0.00044 [kg/s] and (b) mass flow rate: 0.00045 [kg/s]

In this Section the present numerical model (see Section 2.2) is used to predict the capillary tube thermal and fluid-dynamic behavior at the aforementioned challenging conditions.

4.1 Simulations of Negrao and Melo (1999)

Negrao and Melo (1999) carried out a numerical simulation on a concentric capillary-tube/suction-line heat exchanger with HCF-134a. The following geometric conditions were considered: total length 3 m, inlet length 0.6 m, heat exchanger length 2.2 m, capillary tube inner diameter 6.1e-4 m, wall roughness 2.13e-6 m, and suction line inner diameter 7.86e-3 m. The operational conditions were: inlet pressure 13.99 kPa, evaporating temperature -22.9 ºC, suction line inlet temperature -11.2 ºC, and sub-cooling ranging from 0 to 10 ºC. Their investigation revealed that convergence could not be found in the sub-cooling range of 3.9 to 5.8 ºC as shown in Figure 7 (dotted line).

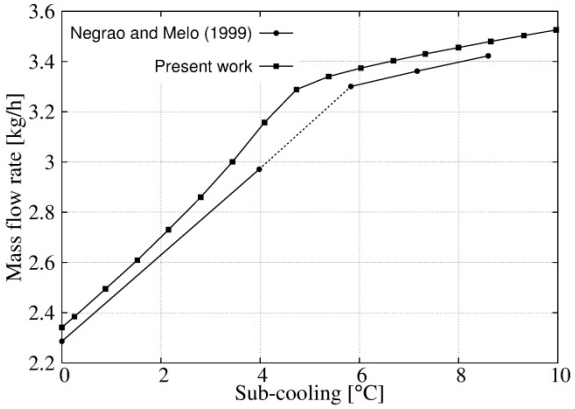

Figure 7: Numerical results of the present model and the model of Negrao and Melo (1999). Dotted line: convergence not attained.

Figure 7 shows that convergence was possible throughout the whole proposed sub-cooling range with the current numerical model. In order to understand and visualize why the sub-cooling range from 3.9 to 5.8 ºC may present convergence issues, the specific case obtained at 4.75 ºC of sub-cooling is studied in detail in Figures 8 and 9.

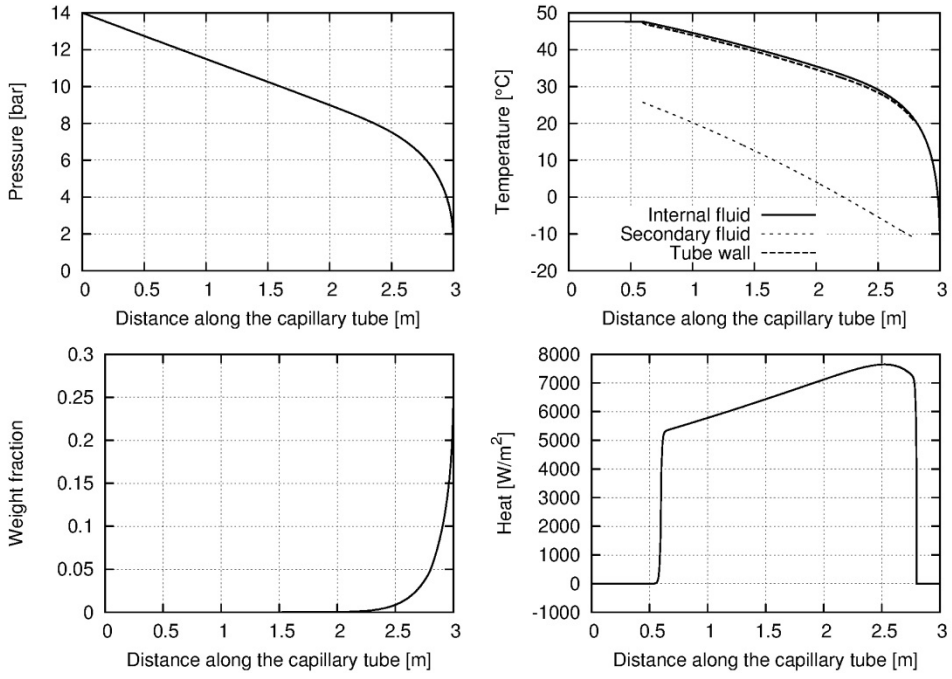

Figure 8: Model predictions of the refrigerant profiles for the non-adiabatic capillary tube presented by Negrao and Melo (1999). Concentric configuration. Sub-cooling of 4.75 ºC.

On one hand Figure 8 shows the pressure, temperature, weight fraction and heat transfer evolutions of the refrigerant along the capillary tube. The temperature and pressure profiles suggest that the typical steep decrease of pressure at the last section of the capillary tube is already happening inside the heat exchanger section. The weight fraction profile indicates that no full re-condensation phenomenon is occurring in this case (i.e. when the refrigerant flow changes from the two-phase condition to the single-phase condition). The smooth heat profile illustrates the effect of the implementations done to the model so that thermal discontinuities are avoided (see Section 2.3). On the other hand the evolution of the refrigerant flow through the capillary tube on a pressure vs. enthalpy diagram is plotted on Figure 9. It is clearly observed that the refrigerant pressure curve is practically following the saturation line for a long distance. This aspect leads to a very unstable situation where the convergence of any distributed model could be seriously affected. Therefore, the possibility to achieve convergence is only possible from a very careful numerical treatment.

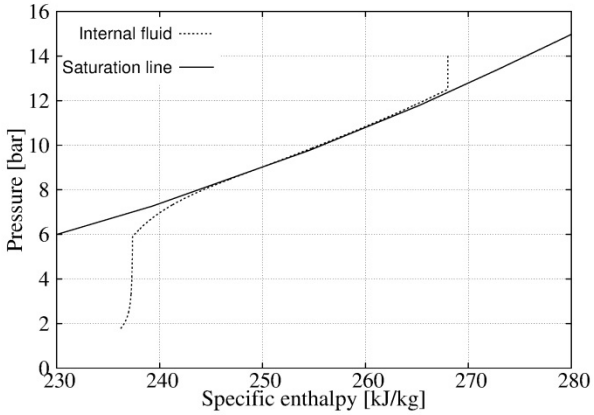

Figure 9: Model predictions of the pressure vs. enthalpy diagram for the non-adiabatic capillary tube of Negrao and Melo (1999). Concentric configuration. Sub-cooling of 4.75 ºC.

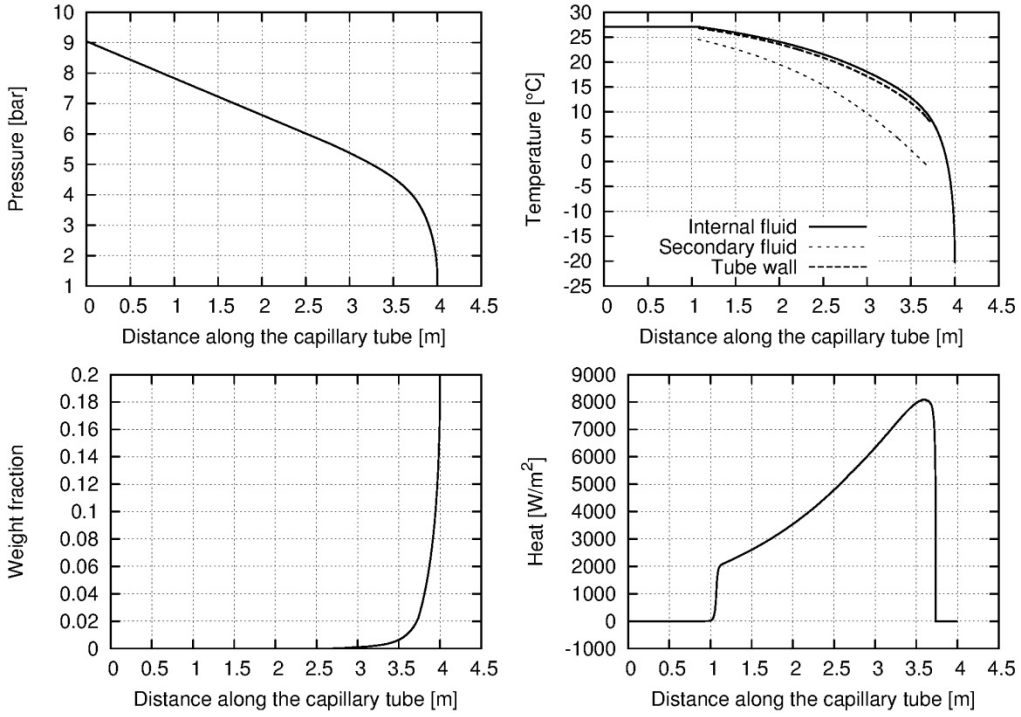

Figure 10: Model predictions of the refrigerant profiles for the non-adiabatic capillary tube of Negrao and Melo (1999). Lateral configuration.

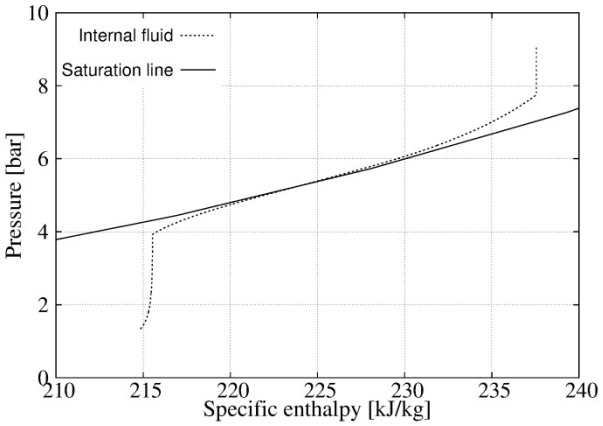

Figure 11: Model predictions of the pressure vs. enthalpy diagram for non-adiabatic capillary tube of Negrao and Melo (1999). Lateral configuration.

Negrao and Melo (1999) have also carried out a numerical simulation on a lateral capillary-tube/suction-line heat exchanger with HFC-134a. The following geometric conditions were considered: total length 4.001 m, inlet length 1.067 m, heat exchanger length 2.670 m, inner diameter 8.3e-4 m, wall roughness 0.58e-6 m, and suction line diameter 7.86e-3 m. The operational conditions were: inlet pressure 9.045 kPa, evaporating temperature -20.3 ºC, suction line inlet temperature -1.6 ºC and sub-cooling degree 8.6 ºC. Similarly to the previous case, their model diverged due to the discontinuities caused by the proximity to the saturation line (and its slope). The results obtained with the present model are plotted in Figures 10 and 11 and show a very similar behavior compared to the previous concentric capillary-tube/suction-line heat exchanger case.

4.2 Simulations of Bansal and Xu (2003)

Bansal and Xu (2003) have numerically investigated the effect of sub-cooling for a lateral capillary-tube/suction-line heat exchanger working with HFC-134a. The following geometrical conditions were considered: total length 1.9 m, inlet length 0.7 m, heat exchanger length 1 m, capillary tube inner diameter 6.6e-4 mm, wall roughness 0.46e-6 m, and suction line internal diameter 6.6e-3 m. The operational conditions were: condensing temperature 34.95 ºC, evaporating temperature -15 ºC, super-heat at suction line inlet 2 ºC and sub-cooling degree from 1 to 3 ºC.

Some numerical convergence difficulties were encountered as the inlet sub-cooling was increased further than 3.5 ºC. Bansal and Xu (2003) realized that these problems were related to the fact that the refrigerant re-condensed within the heat exchanger region and entered to the outlet adiabatic region as sub-cooled liquid, for which the length of the outlet adiabatic section (0.2 m) was not long enough to reach the critical state (they noticed that for longer outlet sections, such as 0.3 m, the convergence problem disappeared).

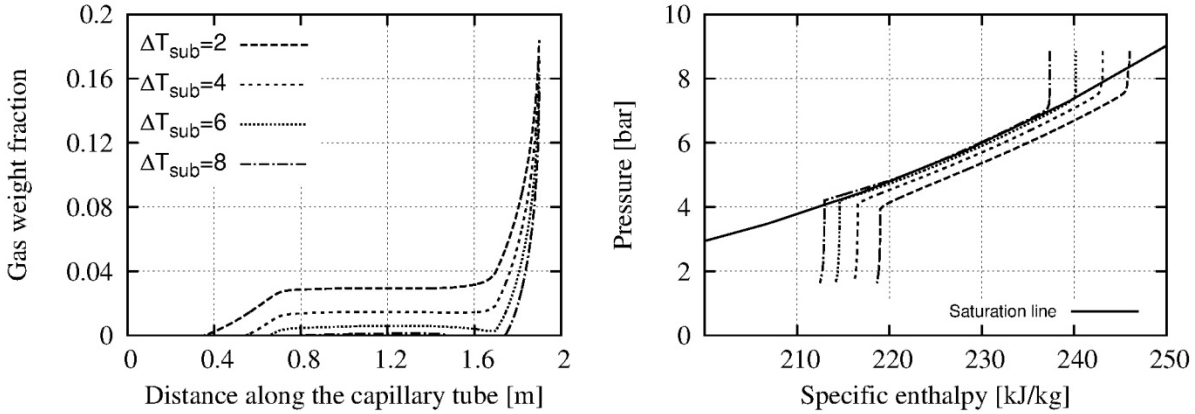

Figure 12: Model predictions of the cases reported by Bansal and Xu (2003).

Figure 12 shows the numerical results obtained with the present model considering the same geometric and operational conditions of Bansal and Xu (2003). In this case the sub-cooling has been varied from 1 to 8 ºC with a step of 0.5 ºC (only 4 cases are presented in the Figure for clarity purposes). As it can be seen convergence has been achieved in the whole range of the studied cases. For the cases below a sub-cooling of 6 ºC the re-condensation phenomenon is not strong enough to drive the refrigerant to the liquid phase. From that sub-cooling value the liquid phase re-appears in the capillary tube. Despite the shortness of the last adiabatic part of the lateral capillary-tube/suction-line heat exchanger the critical state is calculated satisfactorily.

5. CONCLUSIONS

This work reports the major characteristics of an enhanced distributed model that predicts the thermal and fluid-dynamical behavior inside non-adiabatic capillary tubes. On one hand, the lateral configuration has been implemented and validated against experimental data collected from the open literature. In general, good agreement has been found (the concentric configuration has been already validated in a previous work). On the other hand, a common drawback found in this type of models (i.e. numerical convergence issues) has been tackled so that several numerical aspects of the resolution procedure have been changed/modified.

It should be said that experimental cases carried out at the aforementioned unstable conditions are needed in order to fully confirm the fluid behavior in such situations (to the best of the authors' knowledge no experimental studies are reported to the date). In fact, the mentioned conditions could really occur in current refrigeration cycles as they are obtained within common operational conditions and geometric configurations. Therefore, the interest in this topic has significant importance. The distributed models may be time consuming compared to simpler models, but their high level of detail may be of great interest when studying capillary tubes and systems.

NOMENCLATURE

D	diameter	(m)	**Subscripts**		
e	specific energy	(J kg^{-1})	c	kinetic	
g	gravity acceleration	(ms^{-2})	ex	heat exchanger	
h	specific enthalpy	(J kg^{-1})	i	grid position	
L	length	(m)	in	inlet	
$\dot{m}$	mass flow rate	(kg s^{-1})	out	outlet, last section	
p	pressure	(Pa)	p	potential	
$\dot{q}$	heat flux	(Wm^{-2})	sec	secondary flow	
S	cross section	(m^2)	sub	sub-cooling	
s	specific entropy	(J kg^{-1} K^{-1})	**Greek**		
$\dot{s}_{gen}$	generation of entropy	(J K^{-1} m^{-3} s^{-1})	θ	inclination angle	(rad)
T	temperature	(K)	ξ	roughness	(μm)
v	velocity	(m s^{-1})	ρ	density	(kg m^{-3})
z	axial position	(m)	τ	shear stress	(Pa)

REFERENCES

Ablanque N., Rigola J., Pérez-Segarra C.D., Oliva A., 2010, Numerical Simulation of Capillary Tubes. Application to Domestic Refrigeration with Isobutane, *Proceedings of the 13th Int. Ref. and Air Conditioning Conference*, Purdue. West Lafayette.

Bansal P.K., Xu B., 2003, A Parametric Study of Refrigerant Flow in Non-Adiabatic Capillary Tubes, *Applied Thermal Engineering*, vol. 23: p. 397-408.

Bansal P.K., Yang C., 2005, reverse Heat Transfer and Re-Condensation Phenomena in Non-Adiabatic Capillary Tubes, *Applied Thermal Engineering*, vol. 25: p. 3187-3202.

Churchill, S.W., 1977, Frictional Equation Spans All Fluid Flow Regimes, *Chemical Eng.*, vol. 84, no. 24: p. 91-92.

Friedel, L., 1979, Improved Friction Pressure Drop Correlation for Horizontal and Vertical Two-Phase Pipe Flow, *Proc. European Two-Phase Flow Meeting*, Ispra, Italy.

García-Valladares O., 2007, Numerical Simulation of Non-Adiabatic Capillary Tubes Considering Metastable Region. Part II: Experimental Validation, *International Journal of Refrigeration*, vol. 30: p. 654-663.

Gnielinski, V., 1976, New Equations for Heat and Mass Transfer in Turbulent Pipe and Channel Flow, *International Chemical Engineering*, vol. 16, no. 2: p. 359-368.

Khan M.K., Kumar R., Sahoo P.K., 2009, Flow Characteristics of refrigerants flowing through capillary tubes – A Review, *Applied Thermal Engineering*, vol. 29: p. 1426-1439.

Mendoça K.C., Melo C., Ferreira R.T.S., Pereira R.H., 1998, Experimental Study on Lateral Capillary Tube – Suction Line Heat Exchangers, *Proceedings of the 13th Int. Ref. and Air Conditioning Conference*, Purdue, paper 450.

Negrao C.O.R., Melo C., 1999, Shortcomings of the Numerical Modeling of Capillary Tube-Suction Line Heat Exchangers, Numerical Simulation of Capillary Tubes. *Proceedings of the 20th Int. Congress of Refrigeration*, IIR/IIF, Sydney.

Peixoto R.A., 1995, Experimental Analysis and Numerical Simulation of Capillary Tube – Suction Line Heat Exchanger Using Refrigerant HFC-134a. *Proceedings of the 19th Int. Congress of Refrigeration*, The Hague, vol. IIIa, p. 437-444.

Premoli, A., Francesco, D., Prima, A., 1970, An Empirical Correlation for Evaluating Two-Phase Mixture Density Under Adiabatic Conditions, *Proc. European Two-Phase Flow Meeting*, Milan, Italy.

Sarker D., Jeong J.H., 2012, Development of Empirical Correlations for Non-Adiabatic Capillary Tube Based on Mechanistic Model, *International Journal of Refrigeration*, vol. 35, issue 4:p. 974-983 .

Shah, M.M., 1979, A General Correlation for Heat Transfer During Film Condensation Inside Pipes, *International Journal of Heat and Mass Transfer*, vol. 84: p. 547-556.

ACKNOWLEDGEMENT

This work has been partially developed within the research project “Numerical simulation and experimental validation of liquid-vapour phase change phenomena. Application to thermal systems and equipments-II” (ENE2011-28699) of the Spanish Government.